Available online at www.sciencedirect.com
ScienceDirect
Journal of Organometallic Chemistry 692 (2007) 5403–5413
Journal of Organometallic Chemistry
www.elsevier.com/locate/jorganchem

Synthesis, characterization, and reactivity of new types of constrained geometry group 4 metal complexes derived from picolyl-substituted dicarbollide ligand systems

Jong-Dae Lee [a], Young-Joo Lee [b], Ki-Chul Son [b], Won-Sik Han [b], Minserk Cheong [c], Jaejung Ko [b,*], Sang Ook Kang [b,*]

[a] Department of Chemistry, Chosun University, 375 Seosuk, Dong-gu, Gwangju 501-759, Republic of Korea
[b] Department of Chemistry, Korea University, 208 Seochang, Chochiwon, Chung-nam 339-700, Republic of Korea
[c] Department of Chemistry and Research Institute for Basic Sciences, Kyung Hee University, Seoul 130-701, Republic of Korea

Received 11 July 2007; received in revised form 20 August 2007; accepted 23 August 2007
Available online 29 August 2007

Abstract

The syntheses of group 4 metal complexes containing the picolyldicarbollyl ligand $Dcab^{Py}H$ [*nido*-7-$HNC_5H_4(CH_2)$-8-R-7,8-$C_2B_9H_{10}$] (**2**) are reported. New types of constrained geometry group 4 metal complexes $(Dcab^{Py})MCl_2$, $[\{(\eta^5\text{-}RC_2B_9H_9)(CH_2)(\eta^1\text{-}NC_5H_4)\}MCl_2]$ (M = Ti, **3**; Zr, **4**; R = H, **a**; Me, **b**), were prepared by the reaction of **2** with $M(NMe_2)_2Cl_2$ (M = Ti, Zr). The reaction of **2** with $M(NMe_2)_4$ in toluene afforded $(Dcab^{Py})M(NMe_2)_2$, $[\{(\eta^5\text{-}RC_2B_9H_9)(CH_2)(\eta^1\text{-}NC_5H_4)\}M(NMe_2)_2]$ (M = Ti, **5**; Zr, **6**; R = H, **a**; Me, **b**), which readily reacted with Me_3SiCl to yield the corresponding chloride complexes $(Dcab^{Py})MCl_2$ (M = Ti, **3**; Zr, **4**; R = H, **a**; Me, **b**). The structures of the diamido complexes $(Dcab^{Py})M(NMe_2)_2$ (M = Ti, **5**; Zr, **6**) were established by X-ray diffraction studies of **5a**, **5b**, and **6a**, which verified an η^5:η^1-bonding mode derived from the dicarbollylamino ligand. Related constrained geometry catalyst CGC-type alkoxy titanium complexes, $(Dcab^{Py})Ti(O^iPr)_2$ (**7**), were synthesized by the reaction of **2** with $Ti(O^iPr)_4$. Sterically less demanding phenols such as 2-Me-C_6H_4OH replaced the coordinated amido ligands on $(Dcab^{Py})Ti(NMe_2)_2$ (**5a**) to yield aryloxy stabilized CGC complexes $(Dcab^{Py})Ti(OPh^{Me})_2$($Ph^{Me}$ = 2- Me–C_6H_4, **8**). NMR spectral data suggested that an intramolecular Ti–N coordination was intact in solution, resulting in a stable piano-stool structure with two aryloxy ligands residing in two of the leg positions. The aryloxy coordinations were further confirmed by single crystal X-ray diffraction studies on complexes $(Dcab^{Py})Ti(OPh^{Me})_2$ (**8**).

Keywords: Pyridylmethylamino dicarbollyl ligand; Group 4 metal complexes; Constrained geometry catalysts; Olefin polymerization; Intramolecularly coordination; Zwitterionic compound

1. Introduction

The dicarbollide ion is a versatile ligand and an isolobal inorganic analogue of the $C_5H_5^-$ ion [1]. The preparation of constrained geometry catalysts (CGCs) with a dicarbollyl functionality is a promising project, since incorporation of a dicarbollyl fragment into the ligand framework would provide new metal/charge combinations. Therefore, recently developed CGCs containing both π-dicarbollyl and σ-amino or -amido components have attracted considerable attention [2]. As part of our ongoing research into the utility of the dicarbollylamino system in the chemistry of group 4 metals, we became interested in preparing CGC-type complexes as catalyst precursors for olefin polymerization [3]. However, the strong π-donor capability of the dicarbollyl group [4] coupled with the inherent electrophilicity of group 4 metal centers results in the formation of the bis(dicarbollyl) complex rather than the desired mono(dicarbollyl) complex [2b,2e].

* Corresponding author. Tel.: +82 41 860 1334; fax: +82 41 867 5396 (S.O. Kang).
E-mail address: sangok@korea.ac.kr (S.O. Kang).

0022-328X/$ - see front matter © 2007 Elsevier B.V. All rights reserved.
doi:10.1016/j.jorganchem.2007.08.027

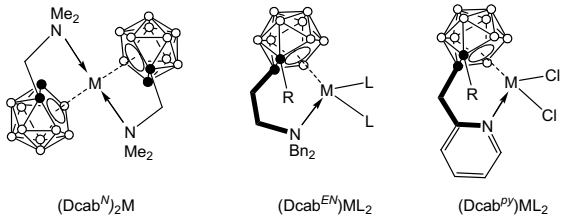

Chart 1. Preference of mono(dicarbollyl) type complexes with a two-carbon spacer.

Recently, we reported a new ligand system ($Dcab^{EN}$) with a two-carbon linker between the central dicarbollyl and the amino group [5], which provides a better coordination environment than that found in the one-carbon-chain homologue ($Dcab^{N}$) for the formation of mono(dicarbollyl) complexes (see Chart 1). Introduction of this two-carbon amine tether enables strong intramolecular interaction with the metal center, thereby favoring the exclusive production of the mono(dicarbollyl) metal complex. In our search for new types of η^5:η^1-coordinating ligand for the production of mono(dicarbollyl) complexes, we introduced a picolyl unit into the dicarbollyl ligand system as a pseudo two-carbon spacer σ-donor. In the present study, we investigated the efficacy of the picolyldicarbollyl ligand as an ancillary ligand system for the generation of mono(dicarbollyl) CGC-type complexes. We found that enhanced σ-donation from the pyridyl unit to the metal center induced a typical η^5:η^1-coordination structure, where constrained geometries were evident in isolated mono(dicarbollyl) complexes [{(η^5-$RC_2B_9H_9$)$(CH_2)_2$(η^1-NC_5H_4)}MCl_2] (M = Ti, **3**; Zr, **4**; R = H, **a**; Me, **b**).

2. Results and discussion

Previously we prepared a series of mono(dicarbollyl) and bis(dicarbollyl) group 4 metal complexes of the type ($Dcab^{N}$)MCl_2 and ($Dcab^{N}$)$_2$MCl (M = Ti, Zr, Hf) [2c,2e], which have a constrained geometry structure around the metal center with η^5:η^1-coordination. We observed that in these ligand systems, the probability of forming the desired mono(dicarbollyl) complex was low except in cases in which specific steric factors intervened. Although coordination of $(Dcab^{N})^{2-}$ reduces the electron count by 2 in theory [6], the thermodynamic driving force behind the formation of the bis(dicarbollyl) complexes is the reduction of the metal's electron deficiency through the formation of the most stable bonding interactions. In another recent study, we reported the exclusive formation of mono(dicarbollyl) complexes ($Dcab^{EN}$)ML_2 [5] when an ethylamine tether was employed as an η^1-amine functionality. These findings indicated that introduction of a two-carbon tether onto the nitrogen atom not only afforded the ideal η^5:η^1-type bonding pocket but also created sufficient steric protection against the association of a second ligand with the metal. Thus, in the present work we incorporated a pseudo two-carbon linker into the dicarbollyl ligand in order to block the formation of bis(dicarbollyl) complexes.

2.1. Picolyldicarbollyl ligand synthesis (*1*)

The ligand **1** was synthesized by a literature procedure [7]. The picolyldicarbollyl ligands, abbreviated as $Dcab^{Py}$H (**2**), were prepared by applying a standard deboronation procedure [8] to 2-pyridylmethyl-*o*-carborane {*closo*-1-(2-NC_5H_4)(CH_2)-2-R-1,2-$C_2B_{10}H_{10}$} (R = H, **1a**; Me, **1b**) (Scheme 1). In this procedure, reaction of **1** with KOH in ethanol at 78 °C and subsequent protonation with phosphoric acid led to the formation of the deboronated zwitterionic compounds **2**.

Spectroscopic characterization of the zwitterionic dicarbollyl ligands **2** showed that the 2-pyridylmethyl group is linked to the *nido* cage carborane. The characteristic asymmetric pattern observed in the $^{11}B\{^1H\}$ NMR spectrum in the range −11 to −38 ppm, and the presence of an absorption at around −3.0 ppm in the ^1H NMR spectrum, imply a B–H–B interaction on the C_2B_3 open face. Most importantly, the methylene protons of the PyCH_2 group each gave rise to an AB spin pattern (3.15, 3.24 (**2a**)/3.25, 3.44 (**2b**) ppm), indicating that they are diastereotopic (Table 1).

2.2. Synthesis and characterization of ($Dcab^{Py}$)ML_2 (M = Ti, Zr; L = Cl, NMe_2) prepared via the amine elimination pathway

The homologous series of picolyldicarbollyl group 4 metal complexes ($Dcab^{Py}$)ML_2 (L = Cl, M = Ti, **3**; Zr, **4**; L = NMe_2, M = Ti, **5**; Zr, **6**) was prepared by reaction of 1:1 mixtures of $Dcab^{Py}$H **2** and $M(NMe_2)_2Cl_2$ or $M(NMe_2)_4$ in toluene at room temperature (Schemes 1 and 2). The overall yields obtained from these reactions typically ranged from 70% to 85%. The ^1H NMR spectra (benzene-d_6) of **5**–**6** exhibited two singlets at 3.25, 3.55 (**5a**), 3.21, 3.59 (**5b**), 3.22, 3.49 (**6a**), and 3.22, 3.51 (**6b**) ppm corresponding to the each methyl protons of the dimethylamido ligands, respectively, due to the asymmetric group 4 metal center. The methylene protons of the PyCH_2 groups in **3**–**6** were diastereotopic, each giving rise to an AB spin pattern. The most significant difference between the ^1H NMR spectra of **3**–**6** and those of the parent ligand

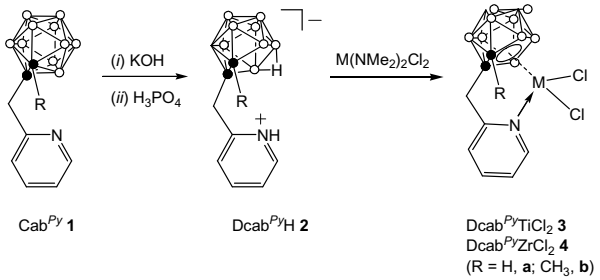

Scheme 1. Synthesis of group 4 metal CGC-type complexes derived from the picolyldicarbollyl ligand **2**.

Table 1
Comparison of the NMR spectroscopic data for compounds **2a**, **2b**, **3a**, **3b**, **4a**, **4b**, **5a**, **5b**, **6a**, **6b**, **7a**, **7b**, and **8**

Compound	$^1H_{CH_2}$	$^1H_{M-NMe_2}$	$^1H_{pyridyl}$	$^1H_{CH_2}$	$^1H_{M-NMe_2}$	$^{13}C_{pyridyl}$
2a[a]	3.15, 3.24		7.92, 8.60, 8.77	56.72		124.76, 127.12, 140.87, 146.17
2b[a]	3.25, 3.44		7.92, 8.62, 8.78	58.90		124.61, 127.56, 140.92, 146.02
3a[c]	3.31, 3.42		6.79, 7.24, 7.57, 8.20	49.23		121.11, 123.09, 130.04, 141.07
3b[c]	3.35, 3.50		6.83, 7.33, 7.67, 8.32	53.37		130.10, 136.83, 143.57, 151.29
4a[c]	3.49, 3.62		6.88, 7.21, 7.59, 8.31	50.29		120.99, 122.48, 129.51, 145.92
4b[c]	3.95, 4.07		6.59, 7.35, 7.76, 8.40	53.17		122.74, 127.45, 133.04, 149.59
5a[c]	2.81, 3.35	3.25, 3.55	7.01, 7.21, 7.82, 8.76	51.74	32.57, 37.49	121.31, 123.57, 142.43, 146.97
5b[c]	3.05, 3.40	3.21, 3.59	7.00, 7.20, 7.88, 8.75	50.91	31.31, 35.74	120.57, 124.08, 142.17, 147.18
6a[c]	2.85, 3.27	3.22, 3.49	7.02, 7.25, 7.81, 8.77	53.49	35.89, 40.52	122.41, 127.88, 141.45, 147.99
6b[c]	3.01, 3.36	3.22, 3.51	7.10, 7.31, 7.84, 8.77	51.85	33.19, 39.67	121.01, 125.48, 142.16, 147.45
7a[b]	3.70, 3.94		7.19, 7.37, 7.93, 8.72	57.55		122.10, 123.63, 141.47, 149.29
7b[b]	3.96, 4.04		7.37, 7.43, 7.95, 8.62	47.83		122.05, 124.39, 141.60, 149.01
8[c]	3.80, 3.94		7.20, 7.34, 7.88, 8.71	56.93		122.29, 125.77, 140.26, 148.97

[a] $(CD_3)_2SO$ was used as the solvent and the chemical shifts are reported relative to the residual H of the solvent.
[b] $CDCl_3$ was used as the solvent and the chemical shifts are reported relative to the residual H of the solvent.
[c] C_6D_6 was used as the solvent and the chemical shifts are reported relative to the residual H of the solvent.

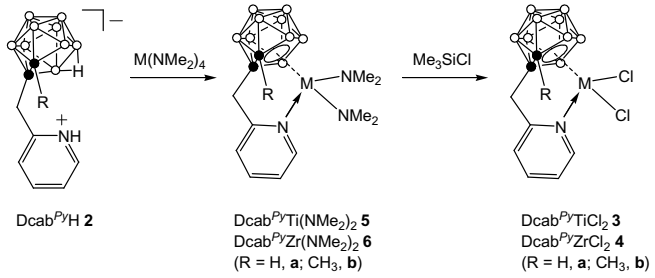

Scheme 2. Alternate synthetic route for the formation of group 4 metal CGC complexes.

systems **2** was a downfield shift of signals for the methylene proton of PyCH_2, from about 3.2 ppm for **2** to 2.81–4.07 ppm for **3**–**6**. The signals for the ring protons on the pyridyl group were also shifted downfield (from 6.59 to 8.77 ppm). These shifts are consistent with similar findings for other intramolecularly coordinated metal complexes containing methylene spacers such as $(Dcab^N)ML_2$, (M = Ti, L = NMe_2 [2c,2e]; M = Fe, Ru, L = Lewis base [9]; M = Ni, L = PPh_3 [10]). In addition, the ^{11}B chemical shifts were similar to those observed for other dicarbollyl metal complexes and support the proposed η^5-coordination [4,11]. The spectroscopic data for complexes **3**–**6** indicated that the 2-pyridylmethyl group of the side chain was coordinated to the metal center in all cases. Compounds **3**–**6** are among the first examples of dicarbollyl group 4 metal complexes with intramolecular coordination of a 2-pyridylmethyl donor function in the side chain.

2.3. Conversion of the $(Dcab^{Py})M(NMe_2)_2$ species to their chloride derivatives

The reactions of **5** and **6** with Me_3SiCl were performed in an effort to produce the corresponding dichloride derivatives (Scheme 2).

The reaction of $(Dcab^{Py})M(NMe_2)_2$ (M = Ti, **5**; Zr, **6**) with 3.3 equiv of Me_3SiCl in CH_2Cl_2 afforded the desired dichloride derivatives, $(Dcab^{Py})MCl_2$ (M = Ti, **3**; Zr, **4**), which were identified by comparison of the chemical shifts of their ^1H and ^{13}C NMR resonances with those measured for authentic samples of **3** and **4**. These metal complexes were purified by low temperature recrystallization from a toluene solution of the mixture.

2.4. Descriptions of the molecular structures of $(Dcab^{Py})Ti(NMe_2)_2$ (**5a**, **5b**) and $(Dcab^{Py})Zr(NMe_2)_2$ (**6a**)

The molecular structures of $(Dcab^{Py})Ti(NMe_2)_2$ (**5**) and the related zirconium bis(dimethylamido) complex $(Dcab^{Py})Zr(NMe_2)_2$ (**6a**) were determined by X-ray crystallography. Important bond distances and angles are shown in Table 2 and selected bond distances and angles are shown in Tables 6 and 7. Perspective views of the molecular structures of compounds **5a**, **5b**, and **6a** are depicted in Figs. 1–3, respectively, along with the non-hydrogen labeling scheme. These compounds exhibit the expected pseudo-tetrahedral geometry consisting of a bi-functional picolyldicarbollyl ligand and two terminal dimethylamido groups.

As shown in Chart 1, the picolyl tethered dicarbollyl ligand ($Dcab^{Py}$) resembles to dicarbollylethylamino ligand ($Dcab^{EN}$) in that both ligand systems contain a two-carbon spacer between η^5:η^1-functionalities. Therefore, direct comparison of important metric parameters regarding the first coordination sphere around the metal center confirms the changes that occurred on the new picolyl-based CGCs **5** and **6**. The overall structural features of the picolyldicarbollyl titanium complex **5a** show some resemblance with those of $(Dcab^{EN})Ti(NMe_2)_2$ (**A**), but the complexes differ substantially in terms of the $Ti–N(1)_{Pyridine}$ distance and α-angle {C_2B_3(centroid)–Ti–$N(1)_{Pyridine}$} associated with the constrained geometry around the titanium metal center (see

Table 2
Compilation of characteristic structural parameters of the **5a**, **5b**, **6a**, **7b**, and **8**[a]

	5a	5b	6a	7b	8	CGC[b]
M–C1	2.424(3)	2.457(7)	2.573(4)	2.416(1)	2.418(4)	
M–C2	2.419(3)	2.476(7)	2.574(4)	2.399(1)	2.388(5)	
M–B9	2.398(4)	2.416(8)	2.512(5)	2.364(1)	2.351(5)	
M–B10	2.419(4)	2.368(8)	2.507(5)	2.355(2)	2.336(5)	
M–B11	2.404(4)	2.420(8)	2.526(5)	2.409(1)	2.370(2)	
M–$Dcab_{(cent)}$	1.940	1.952	2.095	1.916	1.895	2.030
M–N1	2.148(3)	2.160(5)	2.273(3)	2.152(9)	2.101(3)	1.907(3)
M–N2	1.905(3)	1.892(5)	2.015(3)			2.264(1)
M–N3	1.882(3)	1.885(6)	2.018(3)			2.264(1)
$Dcab_{(cent)}$–C1–C3	157.08	159.00	157.83	159.75	159.30	
$Dcab_{(cent)}$–N1	109.29	107.70	103.79	109.37	110.00	107.6
C1–C3-C4	120.2(2)	116.1(6)	116.7(4)	114.2(1)	116.2(3)	
N2–M–N3	101.2(1)	97.8(3)	104.3(2)			102.97(7)
M–O1				1.760(7)	1.785(3)	
M–O2				1.754(7)	1.782(3)	
O1–M–O2				103.3(3)	101.6(1)	

[a] Bond lengths in Å, angles in deg.
[b] $(C_5Me_4)Me_2SiN^tBuTiCl_2$.

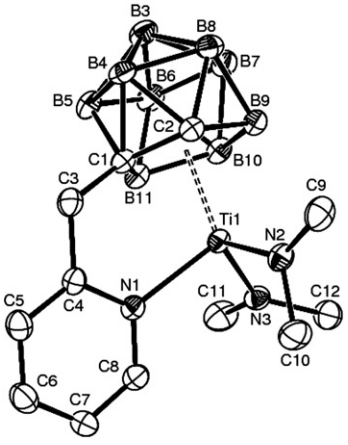

Fig. 1. Molecular structure of **5a** with thermal ellipsoids drawn at the 30% level.

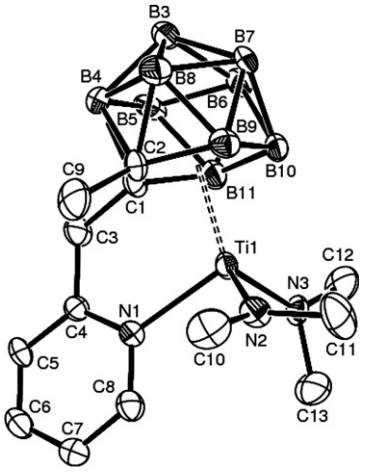

Fig. 2. Molecular structure of **5b** with thermal ellipsoids drawn at the 30% level.

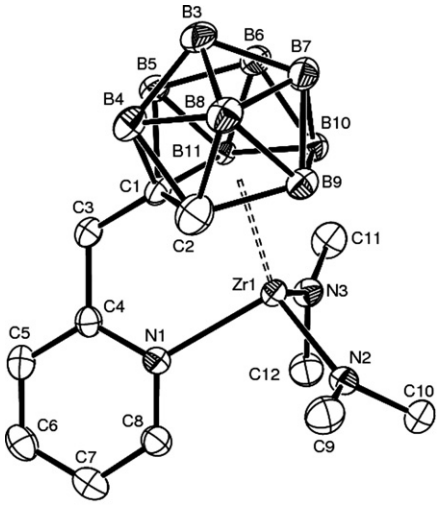

Fig. 3. Molecular structure of **6a** with thermal ellipsoids drawn at the 30% level.

Table 3). The C_2B_3(centroid)–Ti bond distance is similar in **5a** and **A** whereas the Ti–$N(1)_{Pyridine}$ bond distance of 2.148(3) Å for **5a** is considerably shorter than the Ti–$N(1)_{amino}$ distance of 2.319(3) Å for **A**. Strong σ-donation subsequently reduces the corresponding α-angle to 109.3° in comparison with 113.2° for **A**. The remaining metal-amido Ti–N(2)/N(3) distances of 1.894 Å (av.) are similar to those found in complex **A** {1.906 Å (av.)}. Similar structural changes are also found in **5b**, which had a short Ti–$N(1)_{Pyridine}$ distance of 2.160(5) Å and a reduced α-angle, C_2B_3(centroid)–Ti–$N(1)_{Pyridine}$, of 107.70°. Again, this decrease in α-angle is likely due to the enhanced σ-coordination capability of the pyridyl group of the constrained geometry complex [12].

The molecular structure of **6a** manifests constrained geometry structural features similar to those observed in

Table 3
Comparison of bond distances and bond angles for $(Dcab^{EN})Ti(NMe_2)_2$, **5a**, **7b**, and **8**

	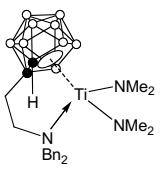 **A**[a]	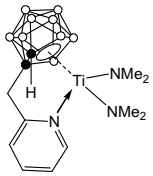 **5a**	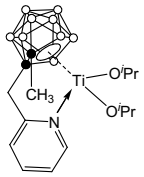 **7b**	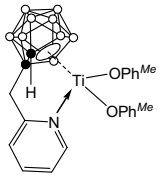 **8**	
Ti–C_2B_3(cent)	1.940 Å	1.940 Å	1.916 Å	1.895 Å	Ti-C_2B_3(cent)
Ti–N(amine)	2.319(3) Å	2.148(3) Å	2.152(9) Å	2.101(3) Å	Ti-N(amine)
Ti-N(amido) (av.)	1.906 Å	1.894 Å	1.757 Å	1.784 Å	Ti–O (Av.)
α-angle[b]	113.2°	109.3°	109.4°	110.0°	α-angle[b]
N(amido)–Ti–N(amido)	101.3°	101.2(1)°	103.3(3)°	101.6(1)°	O–Ti–O
N(amino)–Ti–N(amido) (av.)	77.1°	98.5°	94.9°	94.3°	N(amino)–Ti–O (Av.)

[a] $(Dcab^{EN})Ti(NMe_2)_2$.
[b] C_2B_3(centroid)–Ti–N(amino).

complexes **5**. The $Zr–N(1)_{Pyridine}$ bond distance (2.273(3) Å) in **6a** is slightly longer than the $Ti–N(1)_{Pyridine}$ bond distances in **5** (2.148(3) (**5a**)/2.160(5) (**5b**) Å), and the C_2B_3(centroid)–Zr(1) distance of 2.095 Å in **6a** is slightly longer than the corresponding distances of 1.940 and 1.952 Å in **5a** and **5b**, respectively (see Table 2). The reduced α-angle of 103.8° of **6a** also implies the constrained nature of zirconium complexes [13]. It is evident that the introduction of the pseudo-ethylene linker in the form of a picolyl moiety consistently results in a reduction of the α-angle. Comparison of the structures of two closely related complexes, $(Dcab^{EN})ML_2$ [5] and $(Dcab^{Py})ML_2$, confirmed the significantly constrained nature of the metal center in the picolyldicarbollyl ligand system.

2.5. Synthesis and characterization of $(Dcab^{Py})Ti(OR)_2$ ($R = {}^iPr$, 7; 2-Me-C_6H_4, **8**)

Related aryloxy-substituted picolyldicarbollyl group 4 metal complexes $(Dcab^{Py})Ti(O^iPr)_2$ (**7**) were prepared by reacting 1:1 mixtures of $Dcab^{Py}H$ **2** and $Ti(O^iPr)_4$ in toluene at room temperature (Scheme 3).

As seen above in the amine-elimination reactions of Scheme 2, two O^iPr ligands were easily eliminated from $Ti(O^iPr)_4$ in the presence of the multidentate ligand $Dcab^{Py}H$ (**2**). The signals for the methylene protons of the $PyCH_2$ in **7** were shifted downfield compared to those of the Ti–NMe_2 complexes **5**. The Ti–O^iPr ^1H NMR resonance lines were at 1.40 and 1.47 ppm (**7a**) and 1.38 and 1.43 ppm (**7b**) for [–$CHMe_2$], and at 4.94 and 5.57 ppm (**7a**) and 5.12 and 5.44 ppm (**7b**) for [–$CHMe_2$].

The reaction of $(Dcab^{Py})Ti(NMe_2)_2$ **5a** with 2 equiv of the phenol derivative 2-methylphenol in toluene gave complex **8**. In fact, when **5a** reacted with less hindered phenols such as 2-methylphenol, the expected aryloxy substitution was observed to generate the corresponding bis(aryloxy) stabilized complex $(Dcab^{N})Ti(OPh^{Me})_2$ (Ph^{Me} = 2-Me–C_6H_4, **8**) in high yield (Scheme 4).

The signals from the methylene protons of the $PyCH_2$ in **8** were shifted downfield in comparison with those from the starting material **5a**. The $(Dcab^{Py})Ti(OPh^{Me})_2$ (Ph^{Me} = 2-Me–C_6H_4) complex **8** showed two aryloxy phenyl signals at around 7.12–7.44 ppm and two methyl signals at 2.83 and 3.02 ppm, respectively. The molecular structures of **7b** and **8** were further confirmed by X-ray crystallography (Figs. 4 and 5).

2.6. Description of the molecular structure of $(Dcab^{Py})Ti(O^iPr)_2$ (**7b**) and $(Dcab^{Py})Ti(OPh^{Me})_2$ (Ph^{Me} = 2-Me–C_6H_4) (**8**)

The molecular structures of $(Dcab^{Py})Ti(O^iPr)_2$ (**7b**) and the related titanium aryloxy complex $(Dcab^{Py})Ti(OPh^{Me})_2$ (Ph = 2-Me–C_6H_4) (**8**) were determined by X-ray crystallography. Whereas **7b** was produced via an alkoxy elimination reaction (Scheme 3), **8** was obtained initially from the

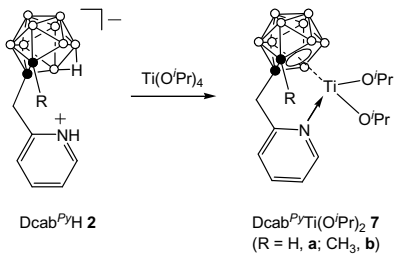

Scheme 3. Synthesis of intramolecularly stabilized titanium alkoxy complexes.

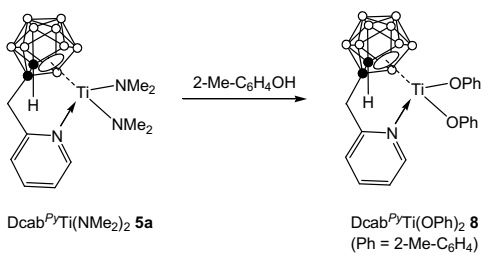

Scheme 4. Reactivity of intramolecularly stabilized titanium aryloxy complexes with 2-methyl phenol.

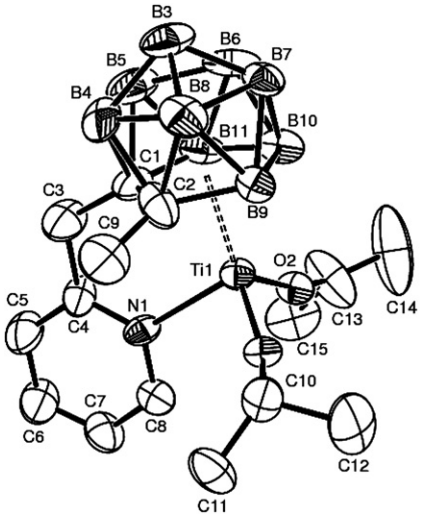

Fig. 4. Molecular structure of **7b** with thermal ellipsoids drawn at the 30% level.

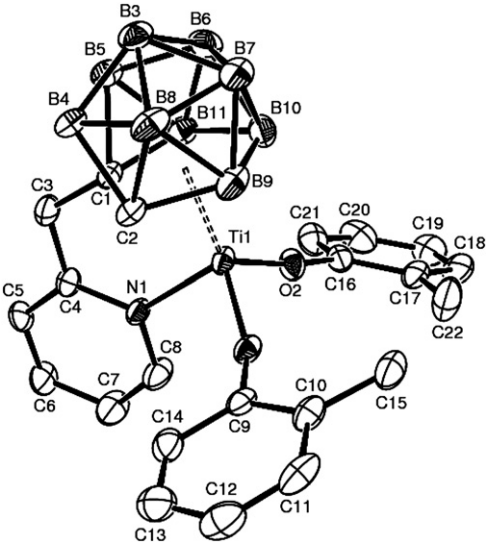

Fig. 5. Molecular structure of **8** with thermal ellipsoids drawn at the 30% level.

reaction of 2.2 equiv of 2-methylphenol with (Dcab^{Py})-Ti(NMe$_2$)$_2$ (**5a**) (Scheme 4). The results of these structural analyses provide the opportunity to evaluate the structural changes due to the replacement of the dimethylamido ligand with an alkoxy or aryloxy ligand.

Perspective views of the molecular structures of **7b** and **8** are shown in Figs. 4 and 5, respectively, along with the non-hydrogen labeling scheme. These compounds exhibit the expected pseudo-tetrahedral geometry, consisting of a bi-functional CGC type ligand and two terminal alkoxy or aryloxy groups. The central titanium atoms in **7b** and **8** are pseudo-tetrahedrally coordinated to a pair of oxo ligands {Ti–O^{i}Pr 1.757 Å (av.), Ti–OPh^{Me} 1.784 Å (av.)}, the pyridine nitrogen, and the dicarbollyl ligand system. The Ti–N(1)$_{Pyridine}$ bond is shorter (2.152(9) (**7b**)/2.101(3) (**8**) Å) than those in complexes **5a** and **5b** (see Tables 2 and 3). The constrained geometry character in a series of related compounds is probably best characterized by the C$_2$B$_3$(centroid)–metal–nitrogen angle, which responds sensitively to steric and electronic geometry changes [14]. In **7b** and **8**, the α angles are 109.4 and 110.0°, which are similar to those found in complexes **5a** and **5b** (108–109°). In contrast, the C$_2$B$_3$(centroid)–Ti bond distances in **7b** and **8** are 1.916 and 1.895 Å, respectively, which are slightly shorter than the corresponding bond distances in complexes **5a** and **5b** (1.94–1.95 Å) (see Table 2).

2.7. Olefin polymerization experiments

Preliminary studies on olefin polymerization were carried out to check whether (Dcab^{Py})MCl$_2$ (M = Ti, **3**; Zr, **4**) and (Dcab^{Py})Ti(OR)$_2$ (R = ^{i}Pr, **7**; 2-MePh, **8**) act as catalyst precursors. These studies revealed that most of the (Dcab^{Py})MCl$_2$ **3**–**4** systems exhibited low activity in ethylene homopolymerization when activated with excess [Ph$_3$C][B(C$_6$F$_5$)$_4$] in cyclohexane at 140 °C under 30 kg/cm^2 of ethylene. The catalytic activities of the **3**/[Ph$_3$C][B(C$_6$F$_5$)$_4$] systems (Table 4, entries 1 and 2) were higher than those of the other studied picolyldicarbollyl complexes, but still much less than that of the prototype Dow-CGC catalyst (Cp*Me$_2$SiN^{t}Bu)TiCl$_2$ (Table 4, entry

Table 4
Ethylene polymerization examples employing the **3a**, **3b**, **4a**, **4b**, **7a**, **7b**, and **8**[a]

Entry	Catalyst	Cocatalyst	Scavenger	Initiation temperature (°C)	Activity[b]	$M_w \times 10^{-4}$[c]	M_w/M_n[c]
1	**3a**	Ph$_3$CB(C$_6$F$_5$)$_4$	mMAO	60	7.9	1.1	2.7
2	**3b**	Ph$_3$CB(C$_6$F$_5$)$_4$	mMAO	60	7.8	0.8	3.1
3	**4a**	Ph$_3$CB(C$_6$F$_5$)$_4$	mMAO	60	5.4	0.8	3.5
4	**4b**	Ph$_3$CB(C$_6$F$_5$)$_4$	mMAO	60	3.7	0.5	3.2
5	**7a**	Ph$_3$CB(C$_6$F$_5$)$_4$	mMAO	60	2.5	0.3	3.5
6	**7b**	Ph$_3$CB(C$_6$F$_5$)$_4$	mMAO	60	2.2	0.3	3.7
7	**8**	Ph$_3$CB(C$_6$F$_5$)$_4$	mMAO	60	1.5	0.1	3.7
8	**Dow-CGC**	Ph$_3$CB(C$_6$F$_5$)$_4$	mMAO	60	26.0	36.7	3.6

[a] Polymerization condition: semi-batch type 500 mL autoclave reactor, solvent = cyclohexane, ethylene pressure = 30 kg/cm^2, total solution volume = 300 mL, catalyst concentration = 3.3 μM, [catalyst]:[cocatalyst]:[scavenger] = 1:1.5:100, reaction time = 10 min.

[b] $\times 10^3$ kg of polymer/(mol of Ti h).

[c] Weight average molecular weight (g/mol) and molecular weight distribution measured by PL210 GPC at 135 °C.

8). The molecular weight distributions obtained from complexes **3** and **4** were in the range of 2.7–3.5. As shown in Table 4, entry 5–7, the alkoxide/aryloxide precursors **7** and **8** showed very low catalytic performance under the stated polymerization conditions.

3. Conclusion

In summary, new types of picolyldicarbollyl group 4 metal complexes were prepared and characterized using ^{1}H, ^{11}B, and ^{13}C NMR spectroscopy as well as X-ray crystallography. The results showed that the picolyldicarbollyl ligand system is an efficient ancillary ligand system for generating mono(dicarbollyl) group 4 metal complexes. The enhanced σ-donation capability of the pyridyl unit allows typical η^5:η^1-bonding around the metal center to construct the constrained geometry in mono(dicarbollyl) complexes. Furthermore, structural studies of the complexes verified the stronger σ-donation of the picolyl tether in $(Dcab^{Py})ML_2$ (M = Ti, Zr) as compared with the related aminoethyl pendant system $(Dcab^{EN})ML_2$ (M = Ti, Zr). Facile ligand substitution reactions with chloride and alkoxide ligands were observed in the titanium-diamido complex $(Dcab^{Py})Ti(NMe_2)_2$ (**5a**). As an application of the newly synthesized constrained geometry complexes, homopolymerization of ethylene was studied in the presence of the picolyldicarbollyl metal complexes. However, in contrast to the prototype Dow-CGC catalyst ($Cp^*Me_2SiN^tBu$)$TiCl_2$, the titanium complexes **3**, **4**, **7**, and **8** exhibited low ethylene polymerization activities.

4. Experimental

4.1. Materials and physical measurements

All manipulations were performed under a dry, oxygen-free nitrogen or argon atmosphere using standard Schlenk techniques or in a Vacuum Atmosphere HE-493 drybox. Toluene, hexane, and pentane were distilled under nitrogen from sodium/benzophenone. Dichloromethane was dried with CaH_2. Benzene-d_6 was distilled under nitrogen from sodium and stored in a Schlenk storage flask until needed. $CDCl_3$ was predried under CaH_2 and vacuum-transferred. *n*-BuLi (2.5 M in hexanes) and $Ti(O^iPr)_4$ were used as received from Aldrich. *o*-Carborane was purchased from KatChem and used after sublimation. The ligand **1** was synthesized by a literature procedure [7]. The starting materials $M(NMe_2)_4$ (M = Ti, Zr) were either purchased from Strem Chemical or prepared by literature methods [15]. All ^{1}H (300.1 MHz, measured in $CDCl_3$), ^{11}B (96.3 MHz, measured in $CDCl_3$) and ^{13}C (75.4 MHz, measured in $CDCl_3$) NMR spectra were recorded on a Varian Mercury-300BB spectrometer unless otherwise stated. ^{1}H and ^{13}C NMR chemical shifts were measured relative to internal residual peaks from the lock solvent (99.5% $(CD_3)_2SO$, 99.9% $CDCl_3$, 99.5% C_6D_6) and then referenced to Me_4Si (0.00 ppm). All ^{11}B NMR chemical shifts were referenced to $BF_3 \cdot O(C_2H_5)_2$ (0.0 ppm) with a negative sign indicating an upfield shift. Elemental analyses were performed using a Carlo Erba Instruments CHNS-O EA1108 analyzer. All melting points were uncorrected.

4.2. Preparation of [nido-7-$HNC_5H_4CH_2$-7,8-$RC_2B_9H_{11}$] (R = H, a; Me, b) (2)

Compound **1a** (0.71 g, 3.0 mmol) and KOH (0.22 g, 4.0 mmol) were dissolved in degassed EtOH (20 mL) and then refluxed under N_2 for 12 h. EtOH was then removed under reduced pressure, and the residue was suspended in benzene (60 mL) and azeotropic distillation was performed to remove H_2O and EtOH. The remaining white solid was dried under vacuum overnight. The solid was slurried in benzene (30 mL) under N_2, H_3PO_4 was added, and the two-phase mixture was stirred vigorously for 15 h. The volatiles were then removed by rotary evaporation under reduced pressure and the residue was washed with H_2O to yield an off-white solid. The product was purified by recrystallization from methanol to yield **2a** (0.55 g, 2.4 mmol) as a colorless crystalline solid in 82% yield. Mp. 172 °C (dec.). Anal. Calc. for $C_8B_9H_{18}N_1$: C, 42.60; H, 8.04; N, 6.21. Found: C, 42.73; H, 8.07; N, 6.23%. ^{11}B NMR (96.3 MHz, DMSO-d_6) δ −12.90 (2B), −16.68 (2B), −22.04 (3B), −34.42 (1B), −38.05 (1B). IR spectrum (KBr pellet, cm^{-1}) ν(B–H) 2543, ν(C–H) 2971, 3015, ν(N–H) 3183.

Compound **2b**: A procedure analogous to the preparation of **2a** was used, but starting from 3.0 mmol (0.75 g) of **1b**. Yield: 92% (0.67 g, 2.8 mmol). Mp. 178 °C (dec.). Anal. Calc. for $C_9B_9H_{20}N_1$: C, 45.12; H, 8.41; N, 5.85. Found: C, 45.28; H, 8.43; N, 5.87%. ^{11}B NMR (96.3 MHz, DMSO-d_6) δ −11.02 (3B), −17.14 (2B), −21.69 (2B), −35.57 (1B), −37.92 (1B). IR spectrum (KBr pellet, cm^{-1}) ν(B–H) 2510, 2555, ν(C–H) 2973, 2991, 3020, ν(N–H) 3166.

4.3. Preparation of ($Dcab^{Py}$)$TiCl_2$ (R = H, a; Me, b) (3)

To a stirred solution of **2a** (0.46 g, 2.0 mmol) in toluene (20 mL) was added a toluene solution of $Ti(NMe_2)_2Cl_2$ (0.50 g, 2.4 mmol) at 0 °C. The mixture was warmed to room temperature and stirred for 1 h. The solvent was then removed under vacuum. Extraction of the residue with toluene (20 mL), followed by concentration to approximately half its volume and cooling to −10 °C, resulted in crystallization of pure **3a** (0.51 g, 1.48 mmol, 74% yield). Anal. Calc. for $C_8B_9H_{16}N_1Ti_1Cl_2$: C, 28.07; H, 4.71; N, 4.09. Found: C, 27.83; H, 4.65; N, 4.01%. ^{11}B NMR (96.3 MHz, benzene-d_6) δ −15.19 (3B), −24.16 (3B), −27.69 (1B), −38.56 (1B), −42.06 (1B). IR spectrum (KBr pellet, cm^{-1}) ν(B–H) 2540, ν(C–H) 2876, 2910.

Compound **3b**: A procedure analogous to the preparation of **3a** was used, but starting from **2b** (0.48 g, 2.0 mmol) in toluene. Yield: 67% (0.48 g, 1.34 mmol). Anal. Calc.f for $C_9B_9H_{18}N_1Ti_1Cl_2$: C, 30.34; H, 5.09; N, 3.93. Found: C,

30.51; H, 5.15; N, 3.99%. ^{11}B NMR (96.3 MHz, benzene-d_6) δ −1.16 (2B), −8.16 (3B), −14.65 (2B), −27.01 (2B). IR spectrum (KBr pellet, cm^{-1}) ν(B–H) 2535, ν(C–H) 2885, 2950.

Compound **4a**: A procedure analogous to the preparation of **3a** was used, but starting from **2a** (0.46 g, 2.0 mmol) in THF. Yield: 81% (0.62 g, 1.62 mmol). Anal. Calc. for $C_8B_9H_{16}N_1Zr_1Cl_2$: C, 24.92; H, 4.18; N, 3.63. Found: C, 25.03; H, 4.22; N, 3.68%. ^{11}B NMR (96.3 MHz, benzene-d_6) δ −15.85 (3B), −21.15 (1B), −24.21 (2B), −26.90 (1B), −38.98 (1B), −42.61 (1B). IR spectrum (KBr pellet, cm^{-1}) ν(B–H) 2514, ν(C–H) 2877, 2955.

Compound **4b**: A procedure analogous to the preparation of **3a** was used, but starting from **2b** (0.48 g, 2.0 mmol) in THF. Yield: 78% (0.62 g, 1.56 mmol). Anal. Calc. for $C_9B_9H_{18}N_1Zr_1Cl_2$: C, 27.05; H, 4.54; N, 3.50. Found: C, 27.19; H, 4.59; N, 3.54%. ^{11}B NMR (96.3 MHz, benzene-d_6) δ −1.65 (2B), −7.67 (3B), −9.94 (3B), −26.84 (1B). IR spectrum (KBr pellet, cm^{-1}) ν(B–H) 2484, 2541, ν(C–H) 2887, 2964.

4.4. Preparation of $(Dcab^{Py})Ti(NMe_2)_2$ (R = H, a; Me, b) (5)

A representative procedure is as follows: over a period of 30 min, a 20 mL toluene solution of $Ti(NMe_2)_4$ (0.22 g, 1.0 mmol) was added to a stirred solution of **2a** (0.23 g, 1.0 mmol) in toluene (20 mL) at 0 °C. After addition was complete, the cold bath was removed and the solution was stirred at room temperature for 1 h. The solvent was then removed under vacuum and the residue was purified by recrystallization with a CH_2Cl_2/toluene mixture at −35 °C. Yield: 87% (0.31 g, 0.87 mmol). Anal. Calc. for $C_{12}B_9H_{28}N_3Ti_1$: C, 40.09; H, 7.85; N, 11.69. Found: C, 39.85; H, 7.76; N, 11.58%. ^{11}B NMR (96.3 MHz, benzene-d_6) δ −9.25 (3B), −10.32 (3B), −16.71 (1B), −28.78 (1B), −34.92 (1B). IR spectrum (KBr pellet, cm^{-1}) ν(B–H) 2540, ν(C–H) 2779, 2961.

Compound **5b**: A procedure analogous to the preparation of **5a** was used, but starting from **2b** (0.24 g, 1.0 mmol). Yield: 88% (0.33 g, 0.88 mmol). Anal. Calc. for $C_{13}B_9H_{30}N_3Ti_1$: C, 41.80; H, 8.09; N, 11.25. Found: C, 42.00; H, 8.20; N, 11.36%. ^{11}B NMR (96.3 MHz, benzene-d_6) δ −5.43 (2B), −15.49 (3B), −17.26 (2B), −29.50 (2B). IR spectrum (KBr pellet, cm^{-1}) ν(B–H) 2553, ν(C–H) 2829, 2957.

Compound **6a** A procedure analogous to the preparation of **5a** was used, but starting from **2a** (0.23 g, 1.0 mmol). Yield: 72% (0.29 g, 0.72 mmol). Anal. Calc. for $C_{12}B_9H_{28}N_4Zr_1$: C, 35.77; H, 7.06; N, 10.43. Found: C, 35.67; H, 6.93; N, 10.32%. ^{11}B NMR (96.3 MHz, benzene-d_6) δ −6.48 (3B), −10.81 (3B), −11.39 (1B), −37.48 (1B), −40.28 (1B). IR spectrum (KBr pellet, cm^{-1}) ν(B–H) 2505, ν(C–H) 2865, 2977.

Compound **6b**: A procedure analogous to the preparation of **5a** was used, but starting from **2b** (1.0 mmol, 0.24 g). Yield: 85% (0.35 g, 0.85 mmol). Anal. Calc. for $C_{13}B_9H_{30}N_3Zr_1$: C, 37.45; H, 7.25; N, 10.08. Found: C, 37.63; H, 7.30; N, 10.16%. ^{11}B NMR (96.3 MHz, benzene-d_6) δ −2.93 (2B), −6.31 (3B), −14.09 (3B), −21.78 (1B). IR spectrum (KBr pellet, cm^{-1}) ν(B–H) 2547, ν(C–H) 2875, 2934.

4.5. Preparation of compound 3 from compound 5

Complex **5a** (0.36 g, 1.0 mmol) was dissolved in CH_2Cl_2 (15 mL), and then an excess amount of Me_3SiCl (3.3 equiv) was added. The resulting solution was stirred for 1 h, after which all volatiles were removed under vacuum and the residue was washed with pentane three times. Removal of the volatiles provided the final crude product, which was further purified from toluene at −15 °C to provide pure complex **3a** as a red solid. Yield: 81% (0.28 g, 0.81 mmol).

Compound **3b**: A procedure analogous to the preparation of **3a** was used, but starting from **5b** (0.37 g, 1.0 mmol). Yield: 68% (0.24 g, 0.68 mmol).

Compound **4a**: A procedure analogous to the preparation of **3a** was used, but starting from **6a** (0.40 g, 1.0 mmol). Yield: 83% (0.32 g, 0.83 mmol).

Compound **4b**: A procedure analogous to the preparation of **3a** was used, but starting from **6b** (0.42 g, 1.0 mmol). Yield: 82% (0.33 g, 0.82 mmol).

4.6. Preparation of $(Dcab^{Py})Ti(O^iPr)_2$ (R = H, **a**; Me = **b**) (7)

To a stirred solution of **2a** (0.23 g, 1.0 mmol) in toluene (20 mL) was added 0.28 g of $Ti(O^iPr)_4$ (1.0 mmol). The mixture was heated at reflux for 12 h, after which the solvent was removed under vacuum and the residue was washed with hexane three times. Removal of the volatiles provided the final crude product, which was further purified by recrystallization from toluene at −35 °C to provide pure complex **7a** as an orange solid. Yield: 77% (0.30 g, 0.77 mmol). Anal. Calc. for $C_{14}B_9H_{30}N_1O_2Ti_1$: C, 43.16; H, 7.76; N, 3.60. Found: C, 43.34; H, 7.80; N, 3.62%. ^{11}B NMR (96.3 MHz, $CDCl_3$) δ 3.68 (1B), −6.73 (1B), −9.47 (2B), −12.89 (2B), −17.71 (2B), −25.56 (1B). IR spectrum (KBr pellet, cm^{-1}) ν(B–H) 2482, 2510, ν(C–H) 2855, 2891, 2952, 3032.

Compound **7b**: A procedure analogous to the preparation of **7a** was used, but starting from **2b** (0.24 g, 1.0 mmol). Yield: 71% (0.29 g, 0.71 mmol). Anal. Calc. for $C_{15}B_9H_{32}N_1O_2Ti_1$: C, 44.64; H, 7.99; N, 3.47. Found: C, 44.81; H, 8.03; N, 3.48%. ^{11}B NMR (96.3 MHz, $CDCl_3$) δ 0.44 (2B), −8.10 (3B), −14.33 (2B), −25.55 (2B). IR spectrum (KBr pellet, cm^{-1}) ν(B–H) 2512, ν(C–H) 2743, 2871, 2922, 3021.

4.7. Preparation of $(Dcab^{Py})Ti[OPh^{Me}]_2$ (R = H) (8)

Compound **5a** (0.36 g, 1.0 mmol) was dissolved in toluene (15 mL), and then an excess amount of 2-Me-C_6H_5OH (2.1 equiv) was added. The reaction mixture was heated at

80 °C for 30 min. Removal of the volatiles provided the final crude product. Extraction of the residue with benzene (10 mL), followed by concentration to approximately half its volume, resulted in crystallization of a pure orange solid. Yield: 93% (0.45 g, 0.93 mmol). Anal. Calc. for $C_{22}B_9H_{30}N_1O_2Ti_1$: C, 54.41; H, 6.23; N, 2.88. Found: C, 54.57; H, 6.24; N, 2.89%. ^{11}B NMR (96.3 MHz, benzene-d_6) δ 2.48 (2B), −0.91 (2B), −14.57 (3B), −27.88 (2B). IR spectrum (KBr pellet, cm^{-1}) ν(B–H) 2492, 2541, ν(C–H) 2888, 2961, 2997, 3038.

4.8. Ethylene homopolymerization

Cyclohexane (300 mL) and mMAO-7 were introduced to a thoroughly dried 500 mL autoclave reactor and the reactor was heated to 140 °C. Specific amounts of catalyst and $[Ph_3C][B(C_6F_5)_4]$ toluene solution were added through a catalyst injector and the reactor was pressurized with ethylene up to 30 kg/cm^2 to start polymerization. During polymerization, the reactor pressure was maintained constant by continuously feeding ethylene. After 10 min, the reactor was cooled to 55 °C, degassed, and 5 mL of acidic ethanol was added to stop the polymerization. The solution was then poured into 1500 mL of ethanol, and the resultant polymer was recovered by filtration and dried *in vacuo* at 70 °C for 12 h.

4.9. Crystal structure determination

Crystals of **5a**, **5b**, **6a**, **7**, and **8** were obtained from toluene, sealed in glass capillaries under argon, and mounted on the diffractometer. Preliminary examination and data collection were performed using a Bruker SMART CCD detector system single-crystal X-ray diffractometer equipped with a sealed-tube X-ray source (40 kV × 50 mA) using graphite-monochromated Mo Kα radiation ($\lambda = 0.71073$ Å). Preliminary unit cell constants were determined with a set of 45 narrow-frame (0.3° in ω) scans. The double-pass method of scanning was used to exclude any noise. The collected frames were integrated using an orientation matrix determined from the narrow-frame scans. The SMART software package was used for data collection, and SAINT was used for frame integration [16a]. Final cell constants were determined by a global refinement of *xyz*

Table 5
X-ray crystallographic data and processing parameters for compounds **5a**, **5b**, **6a**, **7b** and **8**

Compound	**5a**	**5b**	**6a**	**7b**	**8**
Formula	$C_{12}B_9H_{28}N_3Ti$	$C_{13}B_9H_{30}N_3Ti$	$C_{12}B_6H_{28}N_3Zr$	$C_{15}B_9H_{32}NO_2Ti$	$C_{22}B_9H_{31}NO_2Ti$
Formula weight	359.56	373.59	402.88	403.61	486.67
Crystal system	Orthorhombic	Orthorhombic	Orthorhombic	Monoclinic	Monoclinic
Z, Space group	**8**, *Pbca*	**8**, *Pbca*	**8**, *Pbca*	**4**, $P2_1/n$	**4**, $P2_1/c$
a (Å)	14.112(3)	13.517(4)	14.238(1)	11.237(2)	8.045(2)
b (Å)	15.380(3)	15.737(5)	15.324(1)	15.045(3)	25.691(5)
c (Å)	17.476(4)	17.479(4)	17.907(2)	13.309(3)	14.060(3)
V (Å^3)	3793.2(1)	3993.3(2)	3907.1(6)	2227.7(8)	2896.2(9)
μ (mm^{-1})	0.450	0.430	0.562	0.394	0.314
Crystal size (mm)	0.25 × 0.16 × 0.15	0.25 × 0.2 × 0.15	0.2 × 0.17 × 0.16	0.21 × 0.19 × 0.1	0.22 × 0.16 × 0.05
Reflections collected/unique	26573/4726	27754/4969	27440/4854	30165/5547	28699/7181
Reflections observed [$I > 2\sigma(I)$]	1809	621	1704	899	1624
R_{int}	0.1264	0.4803	0.1319	0.3078	0.1348
$R[I > 2\sigma(I)]$, wR_2	0.0513, 0.1088	0.0942, 0.1538	0.0435, 0.0828	0.1604, 0.4057	0.0739, 0.1709
R (all data), wR_2	0.1600, 0.1563	0.3278, 0.2356	0.1371, 0.1144	0.3647, 0.4916	0.1806, 0.2057

Table 6
Selected interatomic distances (Å) for compounds **5a**, **5b**, **6a**, **7b**, and **8**

	5a	**5b**	**6a**	**7b**	**8**	**CGC**
M–C1	2.424(3)	2.457(7)	2.573(4)	2.416(1)	2.418(4)	
M–C2	2.419(3)	2.476(7)	2.574(4)	2.399(1)	2.388(5)	
M–B9	2.398(4)	2.416(8)	2.512(5)	2.364(1)	2.351(5)	
M–B10	2.419(4)	2.368(8)	2.507(5)	2.355(2)	2.336(5)	
M–B11	2.404(4)	2.420(8)	2.526(5)	2.409(1)	2.370(2)	
M–DCab$_{(cent)}$	1.940	1.952	2.095	1.916	1.895	2.030
M–N1	2.148(3)	2.160(5)	2.273(3)	2.152(9)	2.101(3)	1.907(3)
M–N2	1.905(3)	1.892(5)	2.015(3)			
M–N3	1.882(3)	1.885(6)	2.018(3)			
M–N4						
M–O1				1.760(7)	1.785(3)	
M–O2				1.754(7)	1.782(3)	
M–Cl1						2.2635(11)
M–Cl2						2.2635(11)

Table 7
Selected interatomic angles (deg) for compounds **5a**, **5b**, **6a**, **7b**, and **8**

	5a	5b	6a	7b	8	CGC
$DCab_{(cent)}$–C1–C3	157.08	159.00	157.83	159.75	159.30	
N1–M–$DCab_{(cent)}$	109.29	107.70	103.79	109.37	110.00	107.6
C1–C3–N1	120.2(2)	116.1(6)	116.7(4)	114.2(1)	116.2(3)	
N2–M–N3	101.2(1)	97.8(3)	104.3(2)			
O1–M–O2				103.3(3)	101.6(1)	
Cl1–M–Cl2						102.97(7)

centroids of reflections harvested from the entire data set. Structure solution and refinement were carried out using the SHELXTL-PLUS software package [16b]. Detailed information is listed in Tables 5–7.

Acknowledgements

This work was supported by the SRC program of MOST/KOSEF through the Center for Intelligent Nano-Bio Materials at Ewha Womans University (Grant: R11-2005-008-00000-0) and the Korea Research Foundation Grant funded by the Korean Government MOEHRD (KRF-2005-070-C00072) and MOCIE (Contract No. 10016495).

Appendix A. Supplementary material

CCDC 652546, 653245, 652547, 652548, and 652649 contain the supplementary crystallographic data for **5a**, **5b**, **6a**, **7b** and **8**. These data can be obtained free of charge via http://www.ccdc.cam.ac.uk/conts/retrieving.html, or from the Cambridge Crystallographic Data Centre, 12 Union Road, Cambridge CB2 1EZ, UK; fax: (+44) 1223 336 033; or e-mail: deposit@ccdc.cam.ac.uk. Supplementary data associated with this article can be found, in the online version, at doi:10.1016/j.jorganchem.2007.08.027.

References

[1] (a) R.N. Grimes, in: E.W. Abel, F.G.A. Stone, G. Wilkinson (Eds.), Comprehensive Organometallic Chemistry II, Vol. 1, Pergamon, New York, 1995, p. 373;
(b) A.K. Saxena, N.S. Hosmane, Chem. Rev. 93 (1993) 1081–1124.
[2] (a) Y.-J. Lee, J.-D. Lee, J. Ko, S.-H. Kim, S.O. Kang, Chem. Commun. (2003) 1364–1365;
(b) J. Wang, K. Vyakaranam, J.A. Maguire, W. Quintana, F. Teixidor, C. Vioàs, N.S. Hosmane, J. Organomet. Chem. 680 (2003) 173–181;
(c) D.-H. Kim, J.H. Won, S.-J. Kim, J. Ko, S.-H. Kim, S. Cho, S.O. Kang, Organometallics 20 (2001) 4298–4300;
(d) Y. Zhu, K. Vyakaranam, J.A. Maguire, W. Quintana, F. Texidor, C. Vioàs, N.S. Hosmane, Inorg. Chem. Commun. 4 (2001) 486–489;
(e) J.-D. Lee, Y.-J. Lee, K.-C. Son, J. Ko, S.O. Kang, Organometallics 26 (2007) 3374–3384.
[3] (a) A.L. McKnight, R.M. Waymouth, Chem. Rev. 98 (1998) 2587–2598;
(b) Y.-X. Chen, M.V. Metz, L. Li, C.L. Stern, T.J. Marks, J. Am. Chem. Soc. 120 (1998) 6287–6305;
(c) K. Koo, T.J. Marks, J. Am. Chem. Soc. 120 (1998) 4019–4020;
(d) W. Wang, D. Yan, P.A. Charpentier, S. Zhu, A.E. Hamielec, B.G. Sayer, Macromol. Chem. Phys. 199 (1998) 2409–2416;
(e) F. Amor, A. Butt, K.E. du Plooy, T.P. Spaniol, J. Okuda, Organometallics 17 (1998) 5836–5849;
(f) T. Eberle, T.P. Spaniol, J. Okuda, Eur. J. Inorg. Chem. (1998) 237–244;
(g) F. Amor, K.E. du Plooy, T.P. Spaniol, J. Okuda, J. Organomet. Chem. 558 (1998) 139–146;
(h) J. Okuda, T. Eberle, in: R.L. Halterman, A. Tongi (Eds.), Metallocenes, Wiley–VCH, Weinheim, Germany, 1998, p. 415;
(i) Y.-X. Chen, P.-F. Fu, C.L. Stern, T.J. Marks, Organometallics 16 (1997) 5958–5963;
(j) Y. Mu, W.E. Piers, D.C. MacQuarrie, M.J. Zaworotko, V.G. Young, Organometallics 15 (1996) 2720–2726;
(k) K.E. du Plooy, U. Moll, S. Wocadlo, W. Massa, J. Okuda, Organometallics 14 (1995) 3129–3131;
(l) J. Okuda, F.J. Schattenmann, S. Wocadlo, W. Massa, Organometallics 14 (1995) 789–795;
(m) P.J. Shapiro, W.D. Cotter, W.P. Schaefer, J.A. Labinger, J.E. Bercaw, J. Am. Chem. Soc. 116 (1994) 4623–4640;
(n) J.A.M. Canich, U.S. Patent 5,026,798, 1991 (Exxon);
(o) J.C. Stevens, F.J. Timmers, D.R. Wilson, G.F. Schmidt, P.N. Nickias, R.K. Rosen, G.A. Knight, S.Y. Lai, Eur. Pat. Appl. 0416815 A2, 1991 (Dow);
(p) R. Fandos, A. Meetsma, J.H. Teuben, Organometallics 10 (1991) 59–60;
(q) J. Okuda, Chem. Ber. 123 (1990) 1649–1651;
(r) P.J. Shapiro, E. Bunel, W.P. Schaefer, J.E. Bercaw, Organometallics 9 (1990) 867–869.
[4] (a) X. Bei, C. Kreuder, D.C. Swenson, R.F. Jordan, V.G. Young Jr., Organometallics 17 (1998) 1085–1091;
(b) M. Yoshida, R.F. Jordan, Organometallics 16 (1997) 4508–4510;
(c) M. Yoshida, D.J. Crowther, R.F. Jordan, Organometallics 16 (1997) 1349–1351;
(d) D.J. Crowther, D.C. Swenson, R.F. Jordan, J. Am. Chem. Soc. 117 (1995) 10403–10404;
(e) D.E. Bowen, R.F. Jordan, R.D. Rogers, Organometallics 14 (1995) 3630–3635;
(f) C. Kreuder, R.F. Jordan, H. Zhang, Organometallics 14 (1995) 2993–3001;
(g) R. Uhrhammer, Y.-X. Su, D.C. Swenson, R.F. Jordan, Inorg. Chem. 33 (1994) 4398–4402;
(h) G.C. Bazan, W.P. Schaefer, J.E. Bercaw, Organometallics 12 (1993) 2126–2130;
(i) R. Uhrhammer, D.J. Crowther, J.D. Olson, D.C. Swenson, R.F. Jordan, Organometallics 11 (1992) 3098–3104;
(j) D.J. Crowther, N.C. Baenziger, R.F. Jordan, J. Am. Chem. Soc. 113 (1991) 1455–1457.
[5] Y.-J. Lee, J.-D. Lee, H.-J. Jeong, K.-C. Son, J. Ko, M. Cheong, S.O. Kang, Organometallics 24 (2005) 3008–3019.
[6] (a) M.F. Hawthorne, D.C. Young, T.D. Andrews, D.V. Howe, R.L. Pilling, A.D. Pitts, M. Reintjes, L.F. Warren Jr., P. Wegner, J. Am. Chem. Soc. 90 (1968) 879–896;
(b) A. Zalkin, T.P. Hopkins, D.H. Templeton, Inorg. Chem. 6 (1967) 1911–1915;

(c) L. Borodinsky, E. Sinn, R.N. Grimes, Inorg. Chem. 21 (1982) 1686–1689;
(d) R.J. Wilson, L.F. Warren, M.F. Hawthorne, J. Am. Chem. Soc. 91 (1969) 758–759.
[7] (a) E.S. Alekseyeva, A.S. Batsanov, L.A. Boyd, M.A. Fox, T.G. Hibbert, J.A.K. Howard, J.A. Hugh MacBride, A. Mackinnon, K. Wade, Dalton Trans. (2003) 475–482;
(b) X. Wang, G.-X. Jin, Organometallics 23 (2004) 6319–6322.
[8] (a) J. Plesek, S. Hermanek, B. Stibr, Inorg. Synth. 22 (1983) 231–234;
(b) R.A. Wiesboeck, M.F. Hawthorne, J. Am. Chem. Soc. 86 (1964) 1642–1643.
[9] J.-S. Park, D.-H. Kim, J. Ko, S.-H. Kim, S. Cho, C.-H. Lee, S.O. Kang, Organometallics 20 (2001) 4632–4640.
[10] J.-S. Park, D.-H. Kim, S.-J. Kim, J. Ko, S.-H. Kim, S. Cho, C.-H. Lee, S.O. Kang, Organometallics 20 (2001) 4483–4491.
[11] (a) Y.-X. Su, C.E. Reck, I.A. Guzei, R.F. Jordan, Organometallics 19 (2000) 4858–4861;
(b) K.L. Houseknecht, K.E. Stockman, M. Sabat, M.G. Finn, R.N. Grimes, J. Am. Chem. Soc. 117 (1995) 1163–1164;
(c) A.R. Oki, H. Zhang, N.S. Hosmane, Organometallics 10 (1991) 3964–3966;
(d) M.J. Manning, C.B. Knobler, R. Khatter, M.F. Hawthorne, Inorg. Chem. 30 (1991) 2009–2017;
(e) U. Siriwardane, H. Zhang, N.S. Hosmane, J. Am. Chem. Soc. 112 (1990) 9637–9638.
[12] C. Wang, G. Erker, G. Kehr, K. Wedeking, R. Fröhlich, Organometallics 24 (2005) 4760–4773.
[13] (a) G. Lanza, I.L. Fragalà, T.J. Marks, J. Am. Chem. Soc. 122 (2000) 12764–12777;
(b) D.W. Carpendetti, L. Kloppenburg, J.T. Kupec, J.L. Petersen, Organometallics 15 (1996) 1572–1581.
[14] (a) Z. Xie, Coord. Chem. Rev. 231 (2002) 23–46;
(b) M. Gao, Y. Tang, M. Xie, C. Qian, Z. Xie, Organometallics 25 (2006) 2578–2584.
[15] G.M. Diamond, R.F. Jordan, J.L. Petersen, J. Am. Chem. Soc. 118 (1996) 8024–8033.
[16] (a) SMART and SAINT; Bruker Analytical X-ray Division, Madison, WI, 2002;
(b) G.M. Sheldrick, SHELXTL-PLUS Software Package, Bruker Analytical X-ray Division, Madison, WI, 2002.